

ACKNOWLEDGMENTS

The author wishes to thank Professor M. Ueta

for the preparation of CuCl specimens and M. Saito for his help in the experiments.

- ¹M. Cardona, *Phys. Rev.* **129**, 231 (1963).
²T. Ishii, S. Sato, T. Matsukawa, Y. Sakisaka, and T. Sagawa, *J. Phys. Soc. Japan* **32**, 1440 (1972).
³C. Bonnelle, *J. Phys. (Paris)* **28**, C3-65 (1967).
⁴C. Sugiura, *J. Phys. Soc. Japan* **33**, 571 (1972).
⁵S. Sato, T. Ishii, I. Nagakura, O. Aita, S. Nakai, M. Yokota, K. Ichikawa, G. Matsuoka, S. Kono, and T. Sagawa, *J. Phys. Soc. Japan* **30**, 459 (1971).
⁶S. Kono, T. Ishii, T. Sagawa, and T. Kobayashi, *Phys. Rev. Letters* **28**, 1385 (1972).
⁷K. S. Song, *J. Phys. Chem. Solids* **28**, 2003 (1967).
⁸W. W. Beeman, J. Forss, and J. N. Humphrey, *Phys. Rev.* **67**, 217 (1945).
⁹K. Tsutsumi, A. Hayase, and M. Sawada, *J. Phys. Soc. Japan* **12**, 793 (1957).
¹⁰M. Obashi and T. Nakamura, *Japan. J. Appl. Phys.* **10**, 1437 (1971).
¹¹S. Kiyono and C. Sugiura, *Tech. Rep. Tohoku Univ.* **29**, 181 (1964).
¹²M. Ueta and T. Goto, *J. Phys. Soc. Japan* **20**, 401 (1965).
¹³J. A. Bearden, *Rev. Mod. Phys.* **29**, 78 (1967).
¹⁴J. Valasek, *Phys. Rev.* **53**, 274 (1938).
¹⁵C. Sugiura, *J. Phys. Soc. Japan* **32**, 494 (1972).
¹⁶C. Sugiura, *Phys. Rev. B* **6**, 1709 (1972).
¹⁷C. Sugiura (unpublished).
¹⁸C. Sugiura, *J. Chem. Phys.* (to be published).
¹⁹R. D. Deslattes, *Phys. Rev.* **133**, A399 (1964).

Thermodynamic Properties of the Alkali-Halide Crystals*

Francis H. Ree and Albert C. Holt

Lawrence Livermore Laboratory, University of California, Livermore, California 94550

(Received 22 January 1973)

The equilibrium properties of fourteen alkali halides in the NaCl lattice structure are calculated by using an expression for the pair potential given by Tosi and Fumi. The calculations are based on the quasiharmonic lattice-dynamic method and the unsmeared Lennard-Jones-Devonshire cell model. The latter provides numerical estimates of anharmonic contributions which are neglected in the former. Comparison of the calculations with the available experimental data as well as the Monte Carlo data of Woodcock and Singer shows reasonable agreement for the cohesive energy, the pressure, the specific heats, the coefficients of thermal expansion, and the Grüneisen γ 's, but relatively poor agreement in the case of the elastic constants. Our results indicate that the interionic potential for the alkali halides has a stiffer repulsive core and a stronger attractive tail than the expression given by Tosi and Fumi, and that the anharmonic corrections are generally small and should be described accurately by the two lowest terms in a suitable perturbation series. Further discussion is given on the accuracy of using an existing approximate theory for the elastic constants and on the self-consistency of making the quantum and anharmonic corrections introduced here.

I. INTRODUCTION

The alkali-halide crystals hold a certain fascination for experimentalists and theoreticians alike. Theoreticians like them because of their simple crystal structure, because their binding energy is predominantly ionic, and because of the availability of good experimental data. Furthermore, because the NaCl phase is stable over an extended temperature range, and the melting temperature is usually much larger than the Debye temperature, the distinctly anharmonic temperature interval and the distinctly quantum temperature interval are separate, permitting one to exercise and test these aspects of a theoretical model individually. Experimentalists have been attracted to alkali halides because of the availability of large, high-quality single crystals, because of the relative ease of hand-

ling them, and because of the active theoretical interest.

As a result of this interest a large amount of information has been obtained on alkali halides, in view of which it should be possible to determine how well the interionic forces in the alkali halides can be systematically represented by means of two-body central forces which are the sums of contributions from distinct atomic interactions, such as the Coulomb interaction, the van der Waals attraction, and the Born-Mayer repulsion. Fragmentary answers to this question do, in fact, exist. For example, it appears from the work of Szigetti,¹ Lyddane and Herzfeld,² and Lyddane, Sachs, and Teller³ that such a force law cannot reproduce the phonon dispersion curves obtained from neutron scattering data. On the other hand, it is well known⁴ that such an approach does provide a very

useful understanding of lattice spacings and binding energies of salt crystals.

In 1964 Tosi and Fumi,⁵ in the course of deriving new ionic radii based on crystal data and an exponential form for the repulsive energy, obtained a set of interionic potential functions which, to our knowledge, fits reasonably well the whole set of thermodynamic data for salts. In the work described in this paper we have sought to determine where the Tosi-Fumi potential deviates from measured values of the thermodynamic data, including the elastic constants. We have also tried to suggest how the Tosi-Fumi potential might be improved in order to better describe the experimental data.

Given a model for the forces between the ions, several statistical mechanical means are available to compute the equilibrium quantities; namely, the quasiharmonic lattice-dynamic method⁶ with anharmonic contributions obtained from an appropriate perturbation theory, the machine simulations⁷ via the Monte Carlo or the molecular-dynamic method, and the use of a cell model.⁸

The lattice-dynamic method is especially powerful in the temperature-density region where the anharmonic contributions are small but not necessarily the quantum mechanical corrections. Recently, the method has been extensively used to explain the experimental phonon dispersion curves,⁶ and from these studies a great deal of detailed information about the interionic forces has been obtained. However, as mentioned above, no one has been able to explain this information on the basis of a simple force law such as that of Tosi and Fumi, and as a result, increasingly sophisticated models (shell models, breathing shell models, etc.) of the ionic interactions have been developed. Unfortunately these models are sufficiently complicated so that their use in the present work takes up too much computing time. Furthermore, the short-range nature of the interionic interaction force employed in the calculations has remained unchanged from the earlier calculations in that the non-Coulombic forces are confined to first and second neighbors.^{9,10}

At high temperatures or low densities, where the lattice-dynamic method becomes less effective, the computer simulations become most useful. Recently, the Monte Carlo (MC) method was used by Woodcock and Singer¹¹ to compute the liquid-state properties of potassium chloride by means of the Tosi-Fumi potential. They also computed some solid-state data along the 1045 °K isotherm. Their liquid-state data agreed very well with experimental data. The MC data and the experimental data on the melting properties agree reasonably well, considering especially the difficulties in obtaining the experimental data. The observed agreement also suggests that omission of contributions to the potential

energy by the electronic dipoles does not significantly affect the thermodynamic properties.

The anharmonic corrections, which are neglected in the quasiharmonic lattice-dynamic treatment, can be estimated by carrying out analogous calculations using a cell model. Such calculations have been done previously for the rare-gas solids^{12,13} by means of the machine simulations and the Lennard-Jones-Devonshire (LJD) cell model.⁸ Simplified versions of the LJD cell model have also been used by McQuarrie^{14(a)} and Morley.^{14(b)}

In the present work, we have chosen fourteen alkali halides with a NaCl structure and obtained thermodynamic properties by using the Tosi-Fumi potential for these salts. Because of the small ionic radii and the large quantum-mechanical contributions, the Tosi-Fumi potential for lithium halides produced poor thermodynamic results; so we include LiF only to illustrate the difficulties encountered for these cases. Both the quasiharmonic lattice-dynamic method and the LJD cell model were used in the computations. Intermolecular interactions between *all* pairs of ions were included. In addition to trying to determine how well the best pair potential available at present can actually reproduce the experimental thermodynamic data, we have tried to find out how and to what extent the anharmonic terms in the potential energy and the quantum mechanics affect the thermodynamic properties of the alkali halides. In the course of this work, we also learned that the approximate lattice-dynamic treatment of Leibfried and co-workers^{15,16} can lead to qualitatively wrong elastic constants.

The model used in the present work neglects contributions from the dipoles produced by interactions between electrons and between an electron and an ion; nor does it include contributions by three- (or higher-) body forces or noncentral forces. Although it is well known that the electronic-dipole contribution must be included to explain electro-optical effects in crystals, explanation of the thermodynamic data does not necessarily require an explicit consideration of the electronic dipoles or the other factors mentioned above. Inclusion of such factors, moreover, enormously magnifies the computational difficulties. In view of these plus the fact that a satisfactory short-range interaction potential is itself an incompletely understood quantity, we have chosen to leave these factors out entirely in the following considerations.

II. THEORETICAL AND COMPUTATIONAL PROCEDURES

Both the lattice-dynamic and the cell-model expressions for calculating the thermodynamic properties of a single-component system have already been described.¹² These expressions will be used here by modifying them slightly to accommodate a

TABLE I. Parameters in the Tosi-Fumi potential. (Parameters ϵ_{++} , ϵ_{+-} , and ϵ_{--} are equal to 2, $\frac{1}{8}$, and 0.75, respectively, for LiF. For other species, $\epsilon_{++}=1.25$, $\epsilon_{+-}=1$, and $\epsilon_{--}=0.75$. The parameter b is equal to 3.38×10^{-13} erg/molecule. See Ref. 5.)

$$\phi_{ij}(\gamma) = \epsilon_{ij} b e^{(\gamma_i + \gamma_j - \gamma)/\rho} - c_{ij} \gamma^{-6} - d_{ij} \gamma^{-8} + z_i z_j e^2 \gamma^{-1}.$$

The quantity z_i denotes the charge of the i th species in units of an electronic charge (e). Nearest-neighbor distances a at 300°K under zero pressure are also listed.

	r_+ (Å)	r_- (Å)	ρ (Å)	c_{++}	c_{--} (10^{-60} erg cm ⁶)	c_{+-}	d_{++}	d_{--} (10^{-76} erg cm ⁸)	d_{+-}	a (Å) ^a
LiF	0.816	1.179	0.299	0.073	14.5	0.8	0.03	17	0.6	2.0133
NaF	1.170	1.179	0.330	1.68	16.5	4.5	0.8	20	3.8	2.3166
NaCl	1.170	1.585	0.317	1.68	116	11.2	0.8	233	13.9	2.8198
NaBr	1.170	1.716	0.340	1.68	196	14.0	0.8	450	19	2.9887
NaI	1.170	1.907	0.386	1.68	392	19.1	0.8	1100	31	3.2364
KF	1.463	1.179	0.338	24.3	18.6	19.5	24	22	21	2.6736
KCl	1.463	1.585	0.337	24.3	124.5	48	24	250	73	3.1467
KBr	1.463	1.716	0.335	24.3	206	60	24	470	99	3.2984
KI	1.463	1.907	0.355	24.3	403	82	24	1130	156	3.5328
RbF	1.587	1.179	0.328	59.4	18.9	31	82	23	40	2.8257
RbCl	1.587	1.585	0.318	59.4	130	79	82	260	134	3.2904
RbBr	1.587	1.716	0.335	59.4	215	99	82	490	180	3.4478
RbI	1.587	1.907	0.337	59.4	428	135	82	1200	280	3.6755
CsF	1.720	1.179	0.282	152	19.1	52	278	23	78	3.0071

^aNatl. Bur. Stds. (U. S.) Circ. No. 539 (U. S. GPO, Washington, D. C.).

two-component system with Coulomb interactions. We give below an expression for the alkali-halide intermolecular potential and briefly outline the theoretical and computational methods which will be used.

Intermolecular Potential

In 1964, Tosi and Fumi⁵ analyzed the thermodynamic data of the NaCl-type alkali-halide crystals using pair potentials having either an exponential or an inverse-power repulsive core. They conclude that an optimum expression for the pair potential has the following form:

$$\phi_{ij}(\gamma) = \epsilon_{ij} b e^{(\gamma_i + \gamma_j - \gamma)/\rho} - c_{ij} \gamma^{-6} - d_{ij} \gamma^{-8} + z_i z_j e^2 \gamma^{-1}, \quad (1)$$

where the subscript i or j represents a positive or a negative ion. The last term represents the Coulomb potential between two charges $z_i e$ and $z_j e$ separated by a distance γ . The constants c_{ij} and d_{ij} in the attractive parts of $\phi_{ij}(\gamma)$ were determined from ultraviolet-absorption data.¹⁷ Tosi and Fumi's values of the constants ϵ_{ij} , b , γ_i , γ_j , and ρ as well as those of c_{ij} and d_{ij} for fourteen alkali halides investigated here are summarized in Table I. For convenience, the potential given by Eq. (1) will be hereafter referred to as the Tosi-Fumi potential.

Note that the occurrence of a large number of parameters in the Tosi-Fumi potential is somewhat

misleading, since some of these are identical from one salt to another (see Table I). In fact, the total number of independent parameters for seventeen salts (fourteen in Table I plus three lithium salts not studied here) is 105. Hence, on the average, there are about six parameters per alkali halide (or two per ion pair)—a relatively small number considering the complicated appearance of the potential.

Lattice Dynamics

We follow the procedure of Born and von Kármán⁶ and expand the total potential energy of a system of N halogen and N alkali ions, each interacting via the Tosi-Fumi potential [Eq. (1)] in a Taylor series in displacements of the ions from their equilibrium sites. The resulting series is truncated by neglecting terms with third or higher powers in the displacements. The truncated series consists of the static lattice energy (E_0) plus a term quadratic in displacements of the ions. The term linear in displacement drops out on account of the crystal symmetry. Using the periodic boundary condition, the resulting equations of motion for the quasiharmonic Hamiltonian can be diagonalized. This procedure gives $6N-6$ independent normal-mode frequencies ν_i for the $N-1$ wave vectors \vec{y}_i . Because we calculate new coefficients in the expansion for each volume or strained configuration, the vibrational characteristics of the crystal are volume and strain dependent, hence, the term "quasiharmonic."

In the case of ionic crystals, the presence of long-range Coulomb forces makes it impossible to directly apply this procedure. The Coulombic part in the potential energy as well as the corresponding terms in the dynamical matrix must be separately handled either by Evjen's method¹⁸ or by Ewald's method.¹⁹ The former is a direct summation approach which neglects the Coulomb force for $r > \frac{1}{2}L$ (L is the length of the box) or reduces it by a small factor if $r = \frac{1}{2}L$. The latter is an indirect approach which transforms a slowly convergent original Coulomb sum into two rapidly converging sums. We tested the rapidity of convergence of the Coulomb sums by using both the Evjen method and a generalized Ewald's method of Nijboer and de Wette,²⁰ which is applicable to a larger class of lattice sums. The rate of convergence by Evjen's method was slightly slower than that of Ewald's method. To save computing time, Evjen's method, though simpler to treat computationally, was abandoned in favor of Ewald's method.

The normal-mode frequencies (ν_i) for a NaCl structure were evaluated for their Tosi-Fumi potential by a method described in Kellermann's paper.²¹ The Helmholtz free energy (A) can be obtained, in the quasiharmonic approximation, from the knowledge of the ν_i 's, i. e.,

$$A = E_0 + kT \sum_{i=1}^{6N-6} \ln(2 \sinh x_i), \quad x_i = \frac{h\nu_i}{2kT} \quad (2)$$

where h , k , and T denote, respectively, Planck's and Boltzmann's constants, and the absolute temperature. A small contribution of $O(\ln N)$ originating from the center-of-mass motion was left out in Eq. (2).

The internal energy (E) and the constant volume specific heat (C_v) are evaluated, respectively, from the first and second temperature derivatives of Eq. (2) at a fixed volume. To evaluate the pressure P and three isothermal elastic constants C_{11}^T , C_{12}^T , and C_{44} , the procedure of Holt *et al.*¹² is used to relate an initial unstrained position $\vec{x}^0 [\equiv (x_1^0, x_2^0, x_3^0)]$ in the lattice to a new strained position $\vec{x} [\equiv (x_1, x_2, x_3)]$ by means of

$$\begin{aligned} x_1 &= x_1^0(1 + 2\eta_1)^{1/2} \cos \theta, \\ x_2 &= x_1^0(1 + 2\eta_1)^{1/2} \sin \theta + x_2^0(1 + 2\eta_2)^{1/2}, \\ x_3 &= x_3^0, \quad \theta \equiv \sin^{-1} [\eta_6(1 + 2\eta_1)^{-1/2}(1 + 2\eta_2)^{-1/2}], \end{aligned} \quad (3)$$

where η_1 , η_2 , and η_6 are three Lagrangian strain parameters (defined in Fig. 1). These parameters are used to deform the lattice so that strain derivatives can be obtained numerically. The wave vector $\vec{y} [\equiv (y_1, y_2, y_3)]$ corresponding to the deformed lattice is related to the wave vector $\vec{y}^0 [\equiv (y_1^0, y_2^0, y_3^0)]$ of the undeformed lattice by

$$y_1 = [y_1^0 - y_2^0(1 + 2\eta_1)^{1/2}(1 + 2\eta_2)^{-1/2} \sin \theta] /$$

$$(1 + 2\eta_1)^{1/2} \cos \theta, \quad (4)$$

$$y_2 = y_2^0(1 + 2\eta_2)^{-1/2}, \quad y_3 = y_3^0.$$

First, we set $\eta_2 = \eta_6 = 0$ in Eqs. (3) and (4) and numerically evaluate the free energy (2) for three discrete values ($-\Delta\eta, 0, \Delta\eta$) of η_1 . Numerical differentiation of the free energy yields

$$P = V^{-1} \left(\frac{\partial A}{\partial \eta_1} \right)_T, \quad (5)$$

$$C_{11}^T = V^{-1} \left(\frac{\partial^2 A}{\partial \eta_1^2} \right)_T, \quad (6)$$

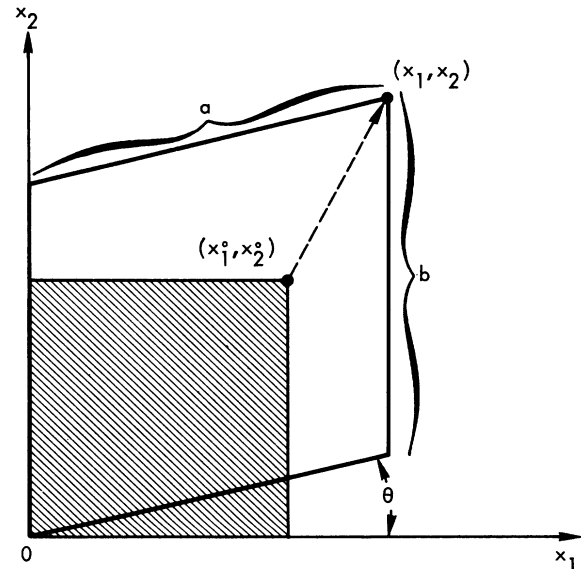
and

$$\Delta C \equiv C_{11}^S - C_{11}^T = C_{12}^S - C_{12}^T = V^{-1} \left(\frac{\partial S}{\partial \eta_1} \right)_T^2 \left(\frac{\partial T}{\partial S} \right)_\eta, \quad (7)$$

where S is the entropy and the superscript S refers to the adiabatic elastic constants. Likewise by evaluating free energies for configurations having two simultaneous strains η_1 and η_2 ($\eta_6 = 0$) and for free energies having a shear strain $\eta_6 \neq 0$ ($\eta_1 = \eta_2 = 0$), we obtain, respectively,

$$C_{12}^T = V^{-1} \left(\frac{\partial^2 A}{\partial \eta_1 \partial \eta_2} \right)_T, \quad (8)$$

$$C_{44} = V^{-1} \left(\frac{\partial^2 A}{\partial \eta_6^2} \right)_T. \quad (9)$$



$$a = x_1^0(1 + 2\eta_1)^{1/2}, \quad b = x_2^0(1 + 2\eta_2)^{1/2}$$

$$\eta_6 = [(1 + 2\eta_1)(1 + 2\eta_2)]^{1/2} \sin \theta$$

FIG. 1. Definitions of the strain parameters η_1 , η_2 , and η_6 , which are used to deform an initial lattice site (x_1^0, x_2^0, x_3^0) to a new position ($x_1, x_2, x_3 = x_3^0$).

The above computing scheme requires several internal parameters (N_s , N_d , N_B , and $\Delta\eta$). The quantities N_s and N_d represent, respectively, the numbers of neighboring shells included in the static lattice sums and the lattice sums in the dynamical matrices. The number N_B represents the number of mesh points in the first Brillouin zone, and the quantity $\Delta\eta$ denotes the differential elements of the strain parameters. For a finite crystal, the numbers N_s , N_d , and N_B are not independent and should be represented by a single parameter. However, since our interest lies in calculations for an infinite-sized system, we chose them independently to achieve faster convergence to the infinite-system values without using unnecessarily large N_s , N_d , or N_B . The final values for N_s and N_d are 8 and 5, respectively, and N_B was chosen to be 499 for the LiF and NaF calculations and 107 for the other calculations. The value for $\Delta\eta$ was set to 0.0001. Test calculations on LiF, NaF, and KF using different values of N_s , N_d , and N_B indicate that the results quoted in Sec. III represent essentially the infinite-system values. In the case of NaF, for example, a test calculation at 295 °K and lattice spacing equal to 2.31655 Å shows that the entropy (S) and specific heat (C_v) are equal to 7.64R and 5.5593R when $N_B = 499$, and to 7.61R and 5.5586R when $N_B = 107$. This represents an error of 0.4% in S and 0.01% in C_v from the $N_B = 499$ data, which are essentially the same as the infinite-system values. Since the heavier-salt data, which have smaller quantum corrections, are still less sensitive to N_B and since the input value of $N_B = 107$ is used only for the heavier-salt calculations, the errors quoted above can be regarded as upper limits on the errors in the heavier-salt calculations. If a higher accuracy is desired, one merely needs to use a larger value of N_B at the expense of an increased computing time. A FORTRAN program written for this purpose takes about 9.3 min of CDC-7600 machine time to generate the thermodynamic quantities for NaCl or heavier-salt calculations and about 37 min for LiF or NaF calculations at each temperature and volume. The large computing time quoted above is required for two reasons. First, evaluation of the thermodynamic quantities outlined above required the Helmholtz free energies of a salt crystal with *eight* different strained crystal shapes. Second, unlike the previous calculations which take into account at most the next-nearest-neighbor short-range interactions representing fourteen neighboring ions, the lattice sums in the dynamical matrices used in the present work include interactions up to the fifth-neighbor shells (or 1330 neighboring ions). Inclusion of further neighboring shells contributes negligibly to the calculated quantities. For those who may later attempt this type of calculation we mention that the

use of the crystal symmetry should reduce (by a factor of 3 or slightly more) the calculation time quoted above, however, at the expense of making the corresponding program somewhat more complicated.

Cell Model

For our calculations we use the LJD cell model described in Ref. 8. In this model, a box containing N alkali and N halogen ions is partitioned into $2N$ cells, each containing only one ion. It is further assumed that each ion interacts with its neighbors which are fixed at their static-lattice sites. The free energy of the cell model is then

$$A = E_0 + A_+ + A_-, \quad (10)$$

$$A_{\pm} = \left(\frac{3}{2}NkT\right) \ln(2\pi m_{\pm} kT/h^2) - NkT \ln \int_{\Delta_{\pm}} d\vec{r} e^{-\delta\phi_{\pm}/kT}, \quad (11)$$

where subscripts + and - represent alkali and halogen ions with their masses m_+ and m_- , respectively. The symbol $\delta\phi_{\pm}$ denotes the difference in the potential energies of a particle at a position \vec{r} inside its cell and at its static-lattice site. Integration in Eq. (11) is confined to a cell volume Δ_+ or Δ_- . We use the parameter δ (in Fig. 2) to vary the sizes of Δ_+ and Δ_- . This parameter and the lattice spacing a define completely the integration limits of Eq. (11); i. e.,

$$\int_{\Delta_+} d\vec{r} = 8 \int_0^{a-\delta} dx \int_0^{\max(a-x, a-\delta)} dy \int_0^{\max(a-y-x, a-\delta)} dz, \quad (12)$$

$$\int_{\Delta_-} d\vec{r} = 8 \int_0^{\delta} dx \int_0^{\delta} dy \int_0^{\delta} dz.$$

At the solid densities, where the calculations were carried out, the Helmholtz free energy is insensitive to a choice of δ , the difference in the free energy being about 0.1%. This is expected, since, at these densities, a particle collides almost entirely with its neighboring particles rather than

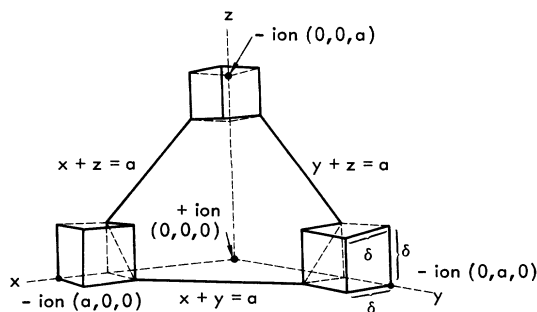


FIG. 2. Shapes of the cell volumes for an alkali ion (at origin) and its three halogen neighbors. This figure represents only one-eighth of the volumes for each type of the ions. The three other halogen neighbors at $(-a, 0, 0)$, $(0, -a, 0)$, and $(0, 0, -a)$ are not shown.

with its cell walls. Therefore, we used a fixed value of $\delta (= 0.5a)$ to obtain the results in Sec. III. The choice of $\delta = 0.5a$ makes both cells look identical, a cube with its sides equal to the lattice spacing. At liquid densities, however, a minimization of the free energy using δ as a variational parameter would likely give improved results on fused salts over those obtained at a fixed δ .

The thermodynamic quantities are obtained by differentiating Eqs. (10) and (11) with respect to the temperature or the strain variables. These expressions were derived earlier¹² for a single-component system and can be directly applied to each of the positive and negative ions in Eq. (10). One modification necessary for the present problem occurs, however, in the evaluation of quantities such as $\sum\phi(r)(x/r)^2$, $\sum\phi(r)(xy/r)^2$, and $\sum\phi(r)(x/r)^4$ for the Coulombic part in the Tosi-Fumi potential. We evaluated them by slightly extending the method of Nijboer and de Wette.²⁰ The summation $\delta\phi_{\pm}$ in the free energy as well as similar terms appearing in the other thermodynamic quantities were calculated by neglecting the contributions beyond the first two neighboring shells of a given ion. Integrations in Eq. (12) were calculated by using the Gauss-Legendre 20-point integration scheme. The infinite-system value of the static-lattice contribution [E_0 in Eq. (10)] can be obtained with sufficient accuracy by including the first eight neighboring shells. Possible errors associated with the above procedure are negligible, and the cell-model results in Sec. III represent the infinite-system values. A computer program for the cell-model thermodynamic quantities took 4.5 min of CDC-7600 machine time for each temperature and volume.

We have also evaluated the thermodynamic quantities (except the elastic constants) from the harmonic cell model. In this case, the Helmholtz free energy is obtained by expanding $\delta\phi_{\pm}$ in Eq. (11) in powers of \tilde{r} and truncating the series after the r^2 term. Since the elastic constants require anisotropic strain derivatives, evaluation of these quantities is more difficult and they have been omitted here. In Sec. III, when they are needed, the harmonic values of the cell-model elastic constants are obtained by extrapolating the difference between the cell-model and static values of the elastic constants [$C_{ij}^T/(\rho kT)$] obtained at a fixed density and at different temperatures to the $T = 0$ value.

III. RESULTS AND DISCUSSION

Comparison with the MC Data

Monte Carlo data with which our results will be compared are the 216-particle data of Woodcock and Singer.¹¹ The interionic potential used by these authors is the Tosi-Fumi potential for potassium

chloride. The solid-state MC data are available only along the 1045°K isotherm. In Table II, these results are shown along with those obtained from the cell model and lattice dynamics at three different molar volumes, i. e., 41.48, 42.70, and 43.92 cm³/mole. Note that the last two volumes lie within the metastable part of the isotherm.

Since the MC data and the theoretical values have identical static-lattice contributions, we only need compare the remaining "thermal" parts. Table II shows that the cell-model values underestimate the MC thermal energies by 5%, 4%, and 5% and overestimate the MC thermal pressures by 3%, 7%, and 8%, respectively, at these volumes. The cell-model approximation as well as the number dependence of the MC data and the "tail correction" made in the MC computations can account for the relatively small errors noted in these quantities. In Table II, the potential energy is further divided into the individual contributions by various parts [Coulomb, (++) , (+-), and (- -) repulsions, r^{-6} and r^{-8} attractions] in the Tosi-Fumi potential. The MC data and the cell-model values agree rather well. Values of the isothermal bulk modulus B_T [$\equiv \frac{1}{3}(C_{11}^T + 2C_{12}^T + P)$], the Grüneisen γ [$\equiv V(\partial P/\partial E)_v$], and coefficient of the volume thermal expansion α_P [$\equiv V^{-1}(\partial V/\partial T)_P = \gamma C_v/VB_T$] are less satisfactory. The exact amount of the deviations which must be attributed to the cell-model approximation cannot be determined at present, since we do not know the errors associated with the MC computations.

Next, we proceed to compare the MC data and the lattice-dynamic results with the reservation that such a comparison will be less meaningful at the melting temperature and at volumes corresponding to metastable states, where one anticipates a sizable anharmonic contribution to a thermodynamic quantity. In the case of the energy, however, this is not so; only 9% of the MC thermal energy can be attributed to the anharmonic effect at the melting point. For the other quantities, the anharmonic contributions are appreciably larger. In particular, the lattice-dynamic values of B_T and the shear modulus $\frac{1}{2}(C_{11}^T - C_{12}^T) - P$ vanish at $V \approx 43.0$ and 42.2 cm³/mole, respectively. The conditions $B_T > 0$, $C_{11}^T > C_{12}^T + 2P$, and $C_{44} - P > 0$ are the so-called Born conditions²² which a crystal must satisfy to maintain stability against mechanical disturbances. It is interesting that the first two Born conditions are violated at volumes inside the metastable region near the MC melting point, where a crystal undergoes a phase change because of a thermodynamic instability. Although closeness of the positions of the two different instabilities is suggestive of a possible relationship between the two as originally conjectured by Born, it may also be entirely an accidental one and might be attributed to the quasiharmonic approximation. In this

TABLE II. Comparison of thermodynamic quantities calculated from the cell-model and the (high-temperature) lattice-dynamic method with Woodcock and Singer's 216-particle Monte Carlo results (Ref. 11) at $T=1045^\circ\text{K}$. Static and thermal contributions to the thermodynamic quantities are separately expressed.

Volume ($\text{cm}^3 \text{mole}^{-1}$) \rightarrow	41.48			42.70			43.92		
	Monte Carlo	Cell model	Lattice dynamics	Monte Carlo	Cell model	Lattice dynamics	Monte Carlo	Cell model	Lattice dynamics
Energy ($10^{10} \text{erg mole}^{-1}$)									
Static	-655.0(2) ^a	-652.6	-650.9	-652.1(2)	-650.3	-648.4	-650.0(4)	-647.8	-645.7
Thermal	-703.0	-703.0	-703.0	-700.6	-700.6	-700.6	-697.9	-697.9	-697.9
	48.0	50.4	52.1	48.5	50.2	52.1	47.9	50.1	52.1
Coulomb	-749.7	-746.1	...	-743.5	-738.9	...	-738.2	-732.0	...
(++) repulsion	1.8	1.5	...	1.6	1.4	...	1.5	1.3	...
(+-) repulsion	95.1	93.2	...	90.3	87.2	...	86.4	81.7	...
(--) repulsion	2.3	1.9	...	2.1	1.7	...	1.9	1.6	...
r^{-6} attraction	-26.5	-25.8	...	-25.4	-24.5	...	-24.4	-23.4	...
r^{-8} attraction	-4.1	-3.4	...	-3.4	-3.2	...	-3.3	-3.0	...
Pressure (10^9dyn cm^{-2})	0.95(8)	0.29	6.83	-1.38(5)	-2.69	5.93	-3.26(11)	-5.18	6.19
Static	-18.51	-18.51	-18.51	-21.04	-21.04	-21.04	-23.09	-23.09	-23.09
Thermal	19.46	18.81	25.34	19.66	18.35	26.97	19.83	17.91	29.27
Isothermal bulk Modulus (10^9dyn cm^{-2})	1.40	1.11	0.48	0.66	0.95	0.13	0.44	0.82	-0.34
Static	0.95	0.95	0.95	0.80	0.80	0.80	0.66	0.66	0.66
Thermal	0.45	0.16	-0.47	-0.14	0.16	-0.67	-0.22	0.16	-1.10
C_p ($J^\circ\text{K}^{-1} \text{mole}^{-1}$)	48(3)	47.1	49.9	48(3)	46.9	49.9	48(3)	45.8	49.9
Grüneisen γ	1.74	1.49	2.02	1.04	1.50	2.21	1.56	1.50	2.47
Coefficient of volume Thermal expansion ($10^{-4}^\circ\text{K}^{-1}$)	1.45	1.53	5.03	2.80	1.73	2.06	3.87	1.95	-8.29

^aNumbers inside parentheses indicate statistical errors; for example, -655.0(2) = -655.0 ± 0.2.

respect, the MC data on the elastic constants along the 1045 °K isotherm, if evaluated, would help resolve the question. Because the cell walls artificially prevent mechanical instabilities from setting in, the cell-model instabilities occur at volumes larger than those quoted in Table II.

Comparison with Experimental Data

The LJD cell model described earlier neglects the quantum-mechanical contributions to the thermodynamic properties. Likewise, the anharmonic contributions are not included in the quasiharmonic lattice-dynamic method. Hence, before proceeding to compare the numerical results with the experimental data, suitable means are desired to correct for these contributions. This can be done most easily by noticing that each of the two models includes a complete account of the corrections missing in the other model. Hence, to make a quantum correction (Δ_{QM}) to an arbitrary thermodynamic quantity F , we add

$$\Delta_{QM} = F(\text{lattice dynamic}) - F(\text{lattice dynamic, classical limit}) \quad (13)$$

to the cell-model value of F . Likewise, to estimate the anharmonic contribution (Δ_{AH}) to F , we use the formula

$$\Delta_{AH} = F(\text{cell model}) - F(\text{harmonic cell model}) \quad (14)$$

and correct the quasiharmonic value of F . The values obtained in this manner will be, hereafter,

referred to as the "quantum cell-model" value and the "anharmonic lattice-dynamic" value, respectively.

At temperatures above about 75% of the melting temperature, where the anharmonic corrections start to become appreciable, Δ_{QM} given by Eq. (13) becomes less reliable. In this case, Δ_{QM} can be neglected entirely because it is a very small number or can be approximated by the first term in the Wigner-Kirkwood expansion,²³ as was done previously.^{12,24,25} The use of the expansion method becomes less reliable at lower temperatures, since the higher-order terms are no longer negligible. As an example, the use of only the first term in the expansion erroneously predicts nearly equal quantum-mechanical contributions to C_{12}^T and C_{44} for the alkali halides and the rare-gas solids.^{12,25} The reliability of estimating the anharmonicity by Eq. (14) deteriorates in a situation where correlated motions of particles must not be ignored. For example, such a situation is present near the melting point in any thermodynamic quantity and in the evaluation of the elastic constants at any temperature. Aside from the limitations noted above, Eqs. (13) and (14) give satisfactory estimates of the corrections, as will be seen in the tables which will be presented later. As a further justification, it can be shown that the lattice-dynamic values in Table II are always improved when the anharmonic corrections are included by Eq. (14).

We shall first compare the experimental and the theoretical thermodynamic data for different alkali

TABLE III. Constant pressure specific heats (C_p) of alkali-halide crystals calculated at 300 °K by the cell-model and the lattice-dynamic methods. Estimates on the quantum and the anharmonic corrections to the cell-model and the lattice-dynamic values, respectively, are listed and included in the theoretical values.

Salts	C_p (J °K ⁻¹ mole ⁻¹)				Expts. ^a	Dev. (%) ^b
	Quantum corrections	Anharmonic corrections	Quantum cell model	Anharmonic lattice dynamics		
LiF	-9.69	-0.44	41.08	43.29	41.90	0.7
NaF	-4.10	-0.55	46.91	51.21	46.82	4.4
NaCl	-2.61	-0.89	48.71	49.16	50.79	-3.7
NaBr	-1.64	-0.99	49.85	50.76	52.30	-3.8
NaI	-1.07	-1.09	50.64	52.54	54.31	-3.2
KF	-2.89	-0.76	48.34	50.76	50.00	-0.9
KCl	-1.54	-1.10	50.14	50.52	51.46	-2.2
KBr	-1.06	-1.03	50.67	50.85	52.51	-3.3
KI	-0.76	-1.10	51.21	51.54	53.22	-3.5
RbF	-2.02	-0.89	49.30	50.45	50.67	-1.6
RbCl	-1.13	-1.28	50.71	50.52	51.21	-1.2
RbBr	-0.67	-0.78	51.36	51.96	51.71	-0.1
RbI	-0.46	-1.13	51.77	51.87	51.80	0.0
CsF	-2.21	-1.25	49.47	49.72	50.66	-2.1

^aLandolt-Börnstein, *Zahlenwerte und Funktionen* (Springer-Verlag, Berlin, 1961), Vol. 2, pt. 4.

^bPercentage deviations between the averaged theoretical values and the experimental data.

TABLE IV. Adiabatic bulk modulus (B_s) of alkali halides at 300 °K. The theoretical values include both the quantum and the anharmonic corrections, whose estimated values are also listed.

Salts	B_s (10^{11} dyne cm^{-2})				Expts. ^{a,b}	Dev. (%) ^c
	Quantum corrections	Anharmonic corrections	Quantum cell model	Anharmonic lattice dynamics		
LiF	0.10	0.00	7.31	9.07	6.77, 6.96	19
NaF	0.02	-0.01	4.03	3.61	4.85, 4.82	-21
NaCl	0.01	-0.01	2.77	2.67	2.46, 2.47	10
NaBr	0.01	0.00	2.09	2.01	2.02, 2.06	0
NaI	0.01	-0.01	1.38	1.30	1.60	-16
KF	0.01	0.00	2.79	2.65	3.17	-14
KCl	0.01	0.00	1.78	1.70	1.80, 1.82	-4
KBr	0.00	-0.01	1.65	1.57	1.53, 1.49	7
KI	0.00	0.00	1.25	1.19	1.21, 1.16	3
RbF	0.01	-0.01	2.65	2.56	2.77	-6
RbCl	0.00	0.00	1.76	1.68	1.65	4
RbBr	0.01	0.00	1.40	1.33	1.37, 1.38	-1
RbI	0.00	0.00	1.19	1.12	1.09, 1.11	5
CsF	0.01	0.00	2.79	2.71

^aLandolt-Börnstein, *Zahlenwerte und Funktionen* (Springer-Verlag, Berlin, 1961), Vols. 1 and 2.

^bG. R. Barsch and Z. P. Chang, *Phys. Status Solidi* **19**, 139 (1967).

^cPercentage deviations between the averaged theoretical values and the averaged experimental data.

halides at 300 °K and at lattice spacings appropriate at one atmospheric pressure (which will hereafter be referred to as zero-pressure situation; see Table I). These values as well as Δ_{QM} and Δ_{AH} are shown in Tables III-V. We note several interesting features in the tables: First, aside from the

three lightest fluorides (LiF, NaF, and KF), the two theoretical values agree with each other reasonably well. This shows a self-consistency in introducing the quantum and the anharmonic corrections by Eqs. (13) and (14). Second, except for LiF and NaF, the averages of the two theoretical

TABLE V. Grüneisen parameters (γ) of alkali halides at 300 °K. The theoretical values include both the quantum and the anharmonic corrections whose values are also listed.

Salts	γ				Expts. ^a	Dev. (%) ^b
	Quantum corrections	Anharmonic corrections	Quantum cell model	Anharmonic lattice dynamics		
LiF	0.17	-0.01	1.27	2.13	1.29	32
NaF	0.06	-0.02	1.19	2.01	1.35	19
NaCl	0.01	-0.03	1.48	1.57	1.56	-2
NaBr	0.01	-0.03	1.47	1.63	1.45	7
NaI	0.01	-0.03	1.42	1.75	1.55	2
KF	0.02	-0.02	1.31	1.78	1.40	10
KCl	0.00	-0.04	1.53	1.58	1.44	8
KBr	0.00	-0.04	1.62	1.58	1.45	10
KI	0.00	-0.04	1.64	1.63	1.56	5
RbF	0.01	-0.03	1.45	1.72	1.50	7
RbCl	0.00	-0.04	1.71	1.64	1.62	3
RbBr	0.00	-0.05	1.70	1.64	1.65	1
RbI	0.00	-0.05	1.81	1.68	1.62	8
CsF	0.00	-0.04	1.83	1.85

^aThese values are computed using the experimental data on C_p (Table III), B_s (Table IV), and the thermal expansion coefficients in Landolt-Börnstein, *Zahlenwerte und Funktionen* (Springer-Verlag, Berlin, 1960), Vol. 2, pt. 2.

^bPercentage deviations between the averaged theoretical values and the experimental data.

TABLE VI. Elastic constants of alkali halides at 300 °K obtained from the LJD cell model, the lattice dynamics, and experiments. Superscript 0 denotes static values of the elastic constants. Thermal parts in the isothermal elastic constants C_{ij}^T are denoted by ΔC_{ij}^T . The adiabatic elastic constants C_{11}^S and C_{12}^S are, respectively, equal to $C_{11}^T + \Delta C$ and $C_{12}^T + \Delta C$.

Salts		Elastic constants (10^{11} erg cm $^{-2}$)						C_{11}^S	C_{12}^S	C_{44}
		C_{11}^0	$C_{12}^0 = C_{44}^0$	ΔC_{11}^T	ΔC_{12}^T	ΔC_{44}	ΔC			
LiF	Cell model	7.91	6.47	0.56	-0.19	0.02	0.18	8.65	6.45	6.48
	Latt. dyn.	7.91	6.47	6.71	-1.16	-0.21	0.57	15.19	5.89	6.25
	Expt. ^a							11.2	4.56	6.32
NaF	Cell model	4.42	3.59	0.37	-0.13	0.01	0.13	4.91	3.59	3.60
	Latt. dyn.	4.42	3.59	-0.49	-0.68	-0.12	0.38	4.31	3.29	3.47
	Expt. ^a							9.70	2.42	2.81
NaCl	Cell model	4.85	1.48	0.13	-0.02	0.02	0.12	5.08	1.58	1.50
	Latt. dyn.	4.85	1.48	-0.16	-0.03	0.01	0.14	4.82	1.58	1.48
	Expt. ^a							4.87	1.26	1.27
NaBr	Cell model	3.43	1.21	0.13	-0.03	0.02	0.11	3.66	1.28	1.24
	Latt. dyn.	3.43	1.21	-0.14	-0.05	0.01	0.13	3.42	1.29	1.22
	Expt. ^a							3.98	1.04	1.00
NaI	Cell model	1.97	0.94	0.13	-0.03	0.02	0.07	2.17	0.98	0.96
	Latt. dyn.	1.97	0.94	-0.11	-0.08	0.00	0.11	1.97	0.98	0.94
	Expt. ^b							3.03	0.89	0.73
KF	Cell model	3.68	2.13	0.23	-0.07	0.03	0.11	4.02	2.17	2.16
	Latt. dyn.	3.68	2.13	-0.20	-0.21	-0.02	0.20	3.68	2.12	2.11
	Expt. ^c							6.50	1.50	1.25
KCl	Cell model	3.23	0.87	0.07	0.00	0.01	0.09	3.40	0.96	0.88
	Latt. dyn.	3.23	0.87	-0.17	-0.01	0.00	0.10	3.17	0.96	0.87
	Expt. ^a							4.06	0.67	0.63
KBr	Cell model	3.22	0.70	0.04	0.01	0.01	0.09	3.35	0.80	0.71
	Latt. dyn.	3.22	0.70	-0.16	0.01	0.00	0.09	3.14	0.79	0.70
	Expt. ^a							3.46	0.56	0.51
KI	Cell model	2.39	0.53	0.04	0.01	0.01	0.08	2.51	0.61	0.54
	Latt. dyn.	2.39	0.53	-0.14	0.00	0.00	0.08	2.33	0.61	0.54
	Expt. ^a							2.74	0.44	0.37
RbF	Cell model	3.99	1.76	0.18	-0.05	0.03	0.11	4.29	1.83	1.80
	Latt. dyn.	3.99	1.76	-0.15	-0.10	0.01	0.16	4.01	1.83	1.77
	Expt. ^d							5.52	1.40	0.93
RbCl	Cell model	3.52	0.69	0.03	0.02	0.01	0.10	3.65	0.81	0.70
	Latt. Dyn.	3.52	0.69	-0.19	0.01	0.00	0.10	3.43	0.80	0.69
	Expt. ^e							3.65	0.65	0.48
RbBr	Cell model	2.76	0.56	0.03	0.01	0.01	0.09	2.87	0.65	0.57
	Latt. dyn.	2.76	0.56	-0.17	0.01	0.00	0.09	2.67	0.65	0.56
	Expt. ^a							3.14	0.48	0.38
RbI	Cell model	2.45	0.42	0.01	0.02	0.01	0.08	2.54	0.52	0.42
	Latt. dyn.	2.45	0.42	-0.16	0.02	0.00	0.07	2.36	0.51	0.42
	Expt. ^a							2.56	0.36	0.28
CsF	Cell model	5.17	1.32	0.10	-0.01	0.04	0.15	5.42	1.47	1.30
	Latt. dyn.	5.17	1.32	-0.16	0.00	0.03	0.16	5.17	1.48	1.35

^aG. R. Barsch and Z. P. Chang, Phys. Status Solidi **19**, 139 (1967).

^bG. R. Barsch and H. E. Shull, Phys. Status Solidi **b43**, 637 (1971).

^cK. M. Koliwad, P. B. Ghate, and A. L. Ruoff, Phys.

Status Solidi **21**, 507 (1967).

^dS. Haussühl, Z. Physik **159**, 223 (1960).

^eM. Ghaflehbashi, D. P. Dandeker, and A. L. Ruoff, J. Appl. Phys. **41**, 652 (1970).

values are close to the corresponding experimental data, the *maximum* deviations being 3.8% for C_p , 16% for B_s , and 10% for the Grüneisen γ .

Third, the quantum cell model describes the thermodynamic properties of LiF very well. The calculated values of C_p , γ , and B_s lie, respectively,

TABLE VII. Values of thermodynamic quantities for potassium chloride at 195 °K, 295 °K, and the melting temperature (T_m) obtained from experiments, the LJD cell model (quantum corrections included), the lattice dynamics (except the elastic constants, the anharmonic corrections included), and the Monte Carlo results (Ref. 11).

	(195 °K, 37.113 cm ³ mole ⁻¹)		(295 °K, 37.515 cm ³ mole ⁻¹)		(T _m =1045 °K, V _m) ^a				
	Expt. ^b	Cell model	Lattice dynamics	Expt. ^b	Cell model	Expt.	Monte Carlo	Cell model	Lattice dynamics
Energy (10 ¹² erg mole ⁻¹)	-6.99 ^c	-6.98 (0) ^e	-6.98 (0) ^f	-6.94 ^c	-6.93 (0)	-6.51 ^d ± 0.02	-6.54 (± 0.00)	-6.56 (0)	-6.56 (0.06)
Pressure (10 ⁹ erg cm ⁻²)	0.00	0.39 (0.27)	0.46 (-0.06)	0.00	0.46 (0.18)	0.00	0.00	7.72 (0.03)	9.96 (-1.40)
C _v (J °K ⁻¹ mole ⁻¹)	46.5	46.1 (-3.2)	46.1 (-0.6)	48.8	47.6 (-1.4)	42-57 ^g	48.4 (± 3)	47.3 (-0.1)	47.3 (-2.5)
C _p (J °K ⁻¹ mole ⁻¹)	47.9	47.5 (-3.5)	47.8 (-0.6)	51.2	50.1 (-1.6)	64-69 ^h	65.3	56.1 (-0.2)	63.8 (-5.1)
Grüneisen γ	1.49	1.53 (0)	1.58 (-0.02)	1.47	1.53 (0)	1.24-1.44 ^s	1.68	1.48 (0)	1.64 (-0.11)
α _p (10 ⁻⁴ °K ⁻¹)	1.01	1.07 (-0.09)	1.13 (-0.03)	1.10	1.14 (-0.04)	1.8-2.4 ⁱ	1.97	1.21 (0)	1.91 (-0.19)
K _T (10 ⁻¹² cm ² erg ⁻¹)	5.42	5.66 (-0.03)	5.84 (0)	5.77	5.92 (-0.02)	10.8 ^j	10.1	6.8 (0)	9.4 (-0.1)
C ₁₁ ^k (10 ¹¹ erg cm ⁻²)	4.38	3.58 (0.02)	3.43	4.05	3.41 (0.01)	1.89 ^j	...	3.08 (0)	2.13
C ₁₂ ^k (10 ¹⁰ erg cm ⁻²)	6.58	9.41 (-0.04)	9.43	6.98	9.53 (-0.02)	7.74 ^j	...	11.04 (0)	10.85
C ₄₄ (10 ¹⁰ erg cm ⁻²)	6.42	8.95 (0.01)	8.86	6.30	8.82 (0.01)	4.85 ^j	...	8.45 (0)	7.94
ΔC (10 ¹⁰ erg cm ⁻²) ^k	0.54	0.57 (-0.04)	0.59 (-0.03)	0.83	0.86 (-0.03)	2.20	...	2.76 (0)	3.50 (-0.59)

^aTheoretical values are calculated at the experimental melting volume (39.16 cm³ mole⁻¹), whereas the Monte Carlo data are those at the MC melting volume (41.75 cm³ mole⁻¹).

^bR. A. Bartels and D. E. Schuele, *J. Phys. Chem. Solids* **26**, 537 (1965).

^cReference 11 for the energy at 295 °K; the energy at 195 °K was obtained by subtracting $\int_{195}^{295} C_p dT$ from the energy at 295 °K, where the data on C_p were taken from W. T. Berg and J. A. Morrison, *Proc. Roy. Soc. A242*, 467 (1970).

^dSee Table IV in Ref. 11.

^eAmount of the quantum-mechanical contribution, which was included in the cell-model value.

^fAmount of the anharmonic contribution, which was included in the lattice-dynamic value.

^gThis is obtained from the experimental data on C_p, α_p, and K_T quoted here.

^hExtrapolated values using the data in F. D. Enck, *Phys. Rev.* **119**, 1873 (1960); and A. J. Leadbetter and G. R. Setliffe, *J. Phys.* **C2**, 385 (1969).

ⁱExtrapolated values using the data in F. D. Enck and J. G. Dommel, *J. Appl. Phys.* **36**, 839 (1965); and A. J. Leadbetter and D. M. T. Newsham, *J. Phys.* **C** **2**, 210 (1969).

^jQ. D. Slagle and H. A. McKinstry, *J. Appl. Phys.* **38**, 437 (1967).

^kΔC ≡ C₁₁^k - C₁₂^k - C₄₄^k.

within 2%, 2%, and 6% of the experimental values. Fourth, the heavier alkali halides have larger anharmonic corrections. This is expected, since the heavier salts have smaller cohesive energies and, as a result, are less tightly bound in the potential well. Both the anharmonic corrections and the quantum corrections reduce the values of C_p , while the values of B_s remain close to the classical harmonic cell-model values on account of a mutual cancellation of the two contributions. More detailed discussion will be given later on the anharmonic effects.

Table VI shows the elastic-constant data obtained from the theories and experiments. The static and the thermal parts in the elastic constants are also separately listed. In contrast to the case for the other thermodynamic properties, agreement between the theories and the experiments are generally poor. The theoretical and experimental values often disagree by 40% or more! These deviations cannot be attributed to the quantum-mechanical and the anharmonic contributions, which are not included in the theoretical values in Table VI. Their contributions are relatively insignificant. The observed deviations occur mainly in the *static-lattice* parts of the elastic constants (see Table VI). This points to the conclusion that the Tosi-Fumi potential is not satisfactory (at least for the elastic constants) to represent a true interionic potential for the alkali halides. A possible way of improving the potential will be discussed later. The thermal contributions to the elastic constants obtained from both theories are in general small. Nevertheless, there are deviations between the two theoretical values, which are mostly attributable to the absence of the cooperative modes in the cell model.

Table VII shows the temperature dependence of the thermodynamic properties of potassium chloride. At 195 and 295 °K, we again note close agreement between the two theoretical values and reasonable agreement (except the elastic constants) between the averages of the two theoretical values and the experimental values. At the melting point, however, Eq. (14) significantly underestimates the true anharmonic corrections because of the enhanced correlated motions of ions. Table VII also lists the MC values¹¹ of the thermodynamic properties. Deviations between those MC data without specified errors and the other data in Table VII should not be regarded as the true differences between the two.

Although the intermolecular potential used in the theoretical calculations is chiefly responsible for the observed deviations in the elastic constants, Figs. 3 and 4 for NaCl and KCl, respectively, show that the qualitative features present in the experimental data are also reproduced in the the-

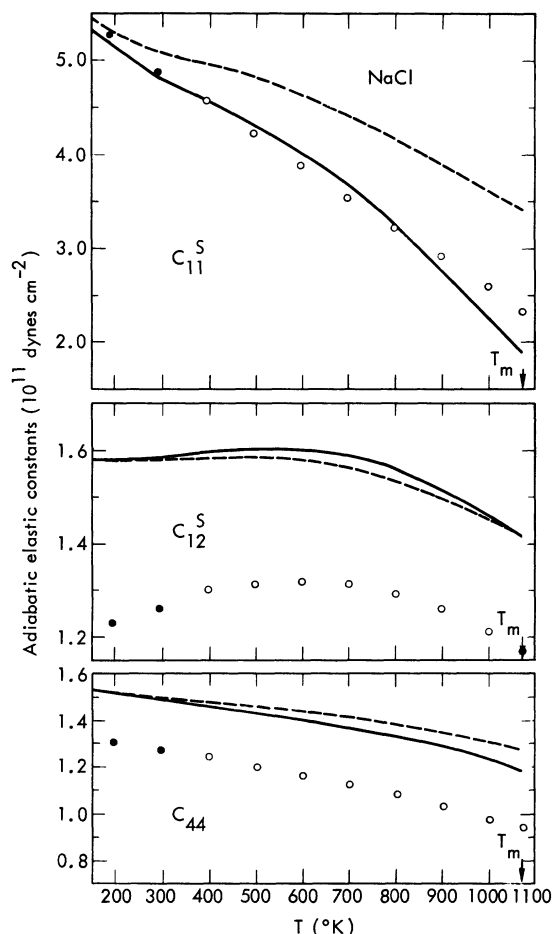


FIG. 3. Adiabatic elastic constants of sodium chloride: black circles, experimental data of Bartels and Schuele [J. Phys. Chem. Solids 26, 537 (1965)]; open circles, experimental data of Slagle and McKinstry [J. Appl. Phys. 38, 437 (1967)]; solid line, the lattice-dynamic calculations; broken line, the cell-model calculations. T_m is the melting temperature.

oretical curves. These are (a) $C_{44}(T) < C_{12}^S(T)$ for $T > 200$ °K and (b) a small positive slope dC_{12}^S/dT for KCl with a peak in C_{12}^S around 800 °K (see also Table VII; the slope for NaCl is positive but smaller). The approximate quasiharmonic theory of Leibfried and co-workers^{15,16} cannot explain both features. In particular, the present data show that it is erroneous to attribute (a) and (b) to many-body forces, as suggested by them. Furthermore, we note that the quasiharmonic thermal contributions (ΔC_{11}^T , ΔC_{12}^T , and ΔC_{44}) calculated by the procedure of Leibfried and co-workers are unacceptably large. For example, the high-temperature calculations on potassium chloride at 295 °K show

$$(\Delta C_{11}^T, \Delta C_{12}^T, \Delta C_{44})/(\rho kT) \\ = (-27.5, -1.9, -0.1)$$

the exact lattice-dynamic values,
 $= (62.5, -27.4, 1.8)$

Leibfried and co-workers's procedure.

These discrepancies originate from an approximation used by Leibfried and co-workers, who replaced each lattice normal-mode frequency by its spectral average $\langle \omega^2 \rangle^{1/2}$ (the Einstein frequency). Numerical values of the elastic constants depend sensitively on the method of evaluating $\langle \omega^2 \rangle$. Leibfried and co-workers evaluated $\langle \omega^2 \rangle$ as the algebraic mean of $\langle \omega_x^2 \rangle$, $\langle \omega_y^2 \rangle$ representing three components of ω^2 . This gives reasonable values of the thermodynamic quantities such as the pressure and the compressibility, which require isotropic strain derivatives of the Helmholtz free energy. But this is not the case for the elastic constants. From his approximate calculations of the elastic constants, Mitskevich²⁶ has also noted this point. The elastic constants require anisotropic strain derivatives, and our calculations on the LJD cell model suggest that the

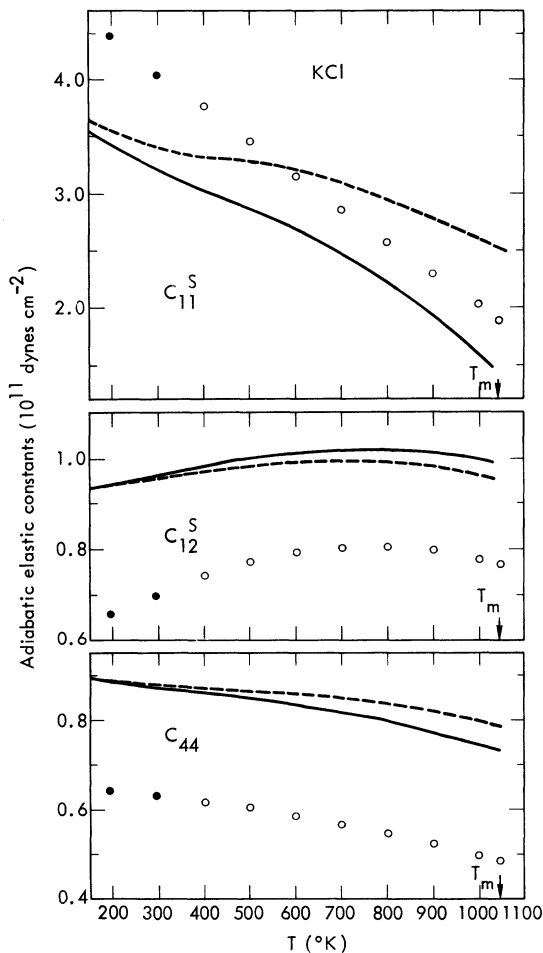


FIG. 4. Adiabatic elastic constants of potassium chloride. See Fig. 3 for the notation.

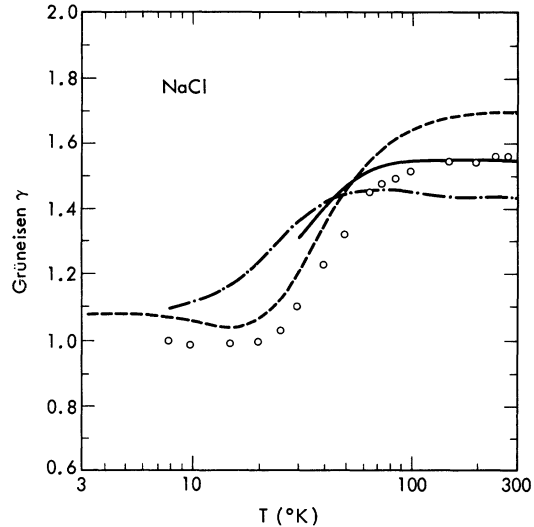


FIG. 5. Temperature dependence of the Grüneisen γ for sodium chloride at constant volume corresponding to 0 °K: circles, experimental points of White (Ref. 28) converted to the constant-volume points by Achar and Barsch (Ref. 27); solid line, the present lattice-dynamic calculations using the Tosi-Fumi potential; dotted line and dashed-dotted line represent, respectively, the shell-model and the modified rigid-ion-model calculations by Achar and Barsch using 0 °K input.

use of $\{[\langle \omega_x^2 \rangle \langle \omega_y^2 \rangle \langle \omega_z^2 \rangle]_{\text{K}} [\langle \omega_x^2 \rangle \langle \omega_y^2 \rangle \langle \omega_z^2 \rangle]_{\text{C1}}\}^{1/6}$ (rather than $\frac{1}{6} \{[\langle \omega_x^2 \rangle + \langle \omega_y^2 \rangle + \langle \omega_z^2 \rangle]_{\text{K}} + [\langle \omega_x^2 \rangle + \langle \omega_y^2 \rangle + \langle \omega_z^2 \rangle]_{\text{C1}}\}$) gives improved values of the elastic constants besides giving correct free energy under the fixed-neighbor ("Einstein") approximation.

At this point we would like to emphasize that the Cauchy conditions would hold in general for two-body central forces only in the static-lattice approximation. Our temperature-dependent two-body central force calculations exhibit features which are qualitatively similar to the deviations from the Cauchy conditions observed in the experimental data. For example, in addition to the effects mentioned above for NaCl and KCl, the 300 °K calculations show a trend from $C_{44} > C_{12}^S$ for the low- Z salts to $C_{12}^S > C_{44}$ for the high- Z salts. The magnitude of the deviations from the Cauchy conditions suggests, as has been repeatedly stated in the literature, that noncentral or many-body forces contribute very little to the elastic constants.

Figure 5 shows the temperature dependence of γ for sodium chloride at a fixed lattice spacing (2.793 Å) appropriate for the 0 °K volume. Theoretical γ 's refer to the lattice-dynamic γ obtained here and to the two others obtained by Achar and Barsch.²⁷ These authors used a six-parameter shell model and a rigid-ion model with first- and second-nearest-neighbor interactions. Experimental values of γ in Fig. 5 are obtained by them

by converting White's²⁸ data at zero pressure to those applicable at the 0 °K volume. Our calculated γ exhibits a shallow maximum ($\gamma = 1.539$) around 250 °K and agrees almost exactly with the experimental γ around 300 °K. At $T = 80$ °K or lower, however, γ 's obtained in this work do not decrease as fast as the experimental values. At $T = 50$ °K or lower, the present calculations, which use 499 wave vectors in the basic Brillouin zone, become less reliable, since a smaller number of the computed frequencies actually contribute to γ by any significant amount. Restrictions on the computing time prevented us from extending the calculations to still lower temperatures, where both the experimental^{28,29} and theoretical studies^{27,30} indicate a shallow minimum in γ . The use of de Launay's formula³¹ gives the 0 °K Debye temperature (Θ_D^0) of 332 °K for sodium chloride compared to the experimental value of 322 °K.²⁵ We evaluated the $\gamma(0 \text{ °K}) = \gamma_0$ from the relation^{30,32} $\gamma_0 = -d \ln \Theta_D^0 / d \ln V$ by a numerical differentiation. The resulting value is about 0.98 ± 0.05 , compared to the experimental value of 1.06 ± 0.01 .²⁹

Anharmonic Contributions

One way of estimating the anharmonic contributions is to develop a perturbation series in the anharmonic parts of the potential energy using the quasiharmonic lattice-dynamic Hamiltonian as the zeroth-order term. The first one or two terms in the expansion can be actually computed in this manner but require very complicated mathematical procedures—an infinite series in the perturbation potential which is in turn an infinite series.^{16,33} On the other hand, the cell-model estimate of the anharmonicity is based on Eq. (14), which is direct and simple and, though less rigorous, has the advantage of estimating a full anharmonic contribution to a thermodynamic quantity. As a result, knowledge of the cell-model anharmonic contributions provides a clue to the rate of convergence of the perturbation series.

In the calculations carried out below, we used potassium chloride as a representative case for all alkali halides studied here (with a possible exception of LiF). To prevent complications arising from the thermal expansion of the lattice, the lattice spacing is fixed at 3.1462 Å, which is the value appropriate to 295 °K and zero pressure. The thermodynamic properties are computed from the cell model at ten different temperatures ranging from 50 to 1000 °K. Within the accuracy of our calculations, these can be fitted by the following quadratic polynomials in T :

$$(A - A_h)/NkT = 1.9 \times 10^{-4} T - 1 \times 10^{-8} T^2, \quad (15a)$$

$$(E - E_h)/NkT = -1.7 \times 10^{-4} T + 3 \times 10^{-8} T^2, \quad (15b)$$

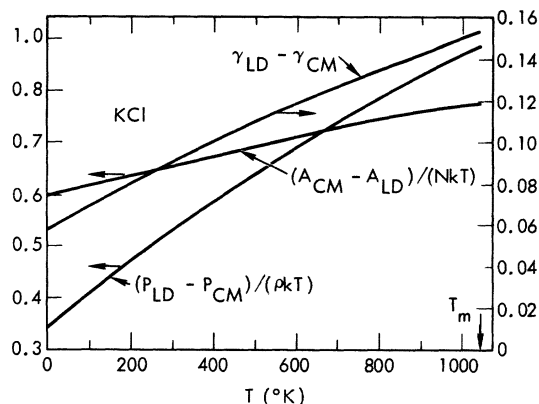


FIG. 6. Differences between the cell-model (CM) and the lattice-dynamic (LD) (classical limit) values of $A(NkT)^{-1}$, $P(\rho kT)^{-1}$, and γ for potassium chloride at different temperatures. The calculations are carried out at constant volume corresponding to 295 °K and zero pressure.

$$(P - P_h)/\rho kT = -6.8 \times 10^{-4} T + 2 \times 10^{-7} T^2, \quad (15c)$$

$$(C_v - C_{vh})/Nk = -3.6 \times 10^{-4} T + 1 \times 10^{-7} T^2, \quad (15d)$$

$$\gamma - \gamma_h = -1.1 \times 10^{-4} T + 2 \times 10^{-8} T^2, \quad (15e)$$

$$(C_{11} - C_{11h})/\rho kT = 3.52 \times 10^{-3} T - 1.0 \times 10^{-6} T^2, \quad (15f)$$

$$(C_{12} - C_{12h})/\rho kT = 8.12 \times 10^{-4} T - 7 \times 10^{-8} T^2, \quad (15g)$$

$$(C_{44} - C_{44h})/\rho kT = 2.16 \times 10^{-5} T + 6 \times 10^{-9} T^2, \quad (15h)$$

where the subscript h denotes the harmonic values obtained by extrapolation to $T \rightarrow 0$ °K. In Eqs. (15a)–(15h) the coefficients of the T^2 terms depend sensitively on the numerical values of the terms linear in T . Hence, they should be regarded as representing only correct orders of magnitude and signs. We note that the sign of the leading anharmonic correction for C_v [Eq. (15d)] does not agree with the one estimated from the experimental data.³⁴ This correction results from the sum of the cubic and quartic terms in the expansion of the potential energy. The two terms contribute nearly equally but have different signs. As a result, the leading anharmonic correction affects only slightly the classical Dulong-Petit value ($6R$); i. e., approximately 2% at room temperature and 6% at the melting point. Therefore, a possible reason for the different signs may lie in our use of the Tosi-Fumi potential, which may be inadequate to explain data on C_v for KCl. (A similar analysis for NaCl gives a consistent result in this respect.) For a more complete explanation, however, it is necessary to carry out first-order perturbation calculations to eliminate an additional contribution arising from the cell-model assumption employed here.

Figure 6 shows the temperature dependence of

the Helmholtz free energy, the pressure, and the Grüneisen γ [Eqs. (15a), (15c), and (15d)]. This figure and Eqs. (15a)–(15h) show that the anharmonicity makes, in fact, very small contributions to the thermodynamic variables. At 1000 °K, which is close to the melting temperature (1045 °K), the anharmonic contributions to A , E , P , etc. [Eqs. (15a)–(15h)] are, respectively, 0.25% (A), -0.2% (E), -8.3% (P), -4.4% (C_v), -6.1% (γ), 1.6% (C_{11}^T), 1.9% (C_{12}^T), and 0.1% (C_{44}). Dominant parts of the anharmonic corrections originate from the terms linear in T in Eqs. (15a)–(15h). Contributions of the second term (proportional to T^2) are $O(10^{-4}T)$ or less, which amounts at most to 10% of the leading terms at the melting point.

Cowley⁹ used a shell model with nearest-neighbor repulsive interactions and computed the first term on the right-hand side of Eq. (15a) from the perturbation theory. The numerical value of the term was found to be small owing to a nearly complete cancellation between the two contributing factors; i. e., the cubic and the quartic terms in the Taylor series expansion of the potential energy. His results for sodium chloride are in qualitative agreement with the present potassium chloride results. From the present results, we can draw the tentative conclusion that the thermodynamic quantities obtained from the perturbation expansion will converge very rapidly for the alkali halides, and that inclusion of the first- and second-order terms [proportional to T^2 in Eqs. (15)] will be sufficient to explain nearly all of the anharmonic contributions to the thermodynamic quantities.

The above conclusion is based on the use of the cell-model approximation. Consequently, one might question how that approximation affects our analysis. Numerical evidence in favor of using these procedures has already been described. Further evidence can be obtained by finding out how adequately the harmonic cell model can approximate the lattice-dynamic results. Our nu-

merical results on the quantities given by Eqs. (15a)–(15e) are encouraging; i. e., the difference between the harmonic cell-model and the lattice-dynamic values are 0.6 for A/NkT , -0.34 for $P/\rho kT$, and -0.06 for γ . (Note that these are represented by the intercepts in Fig. 6. The values of E and C_v agree, of course, exactly.) The elastic constants [Eqs. (15f)–(15h)] have larger deviations, i. e., 37.3 for $C_{11}^T/\rho kT$, 1.00 for $C_{12}^T/\rho kT$, and 2.3 for $C_{44}/\rho kT$. This suggests that the estimates of the anharmonicity become less reliable for the elastic constants in agreement with our earlier discussion. Since the anharmonic contributions affect the elastic constants by less than 3% at any temperature, their estimates based on the cell model may, however, not be too bad in practice.

Analysis of the Tosi-Fumi Potential

We have already noted that the cause of large deviations between the theoretical and the experimental values of the elastic constants lies in the inadequacy of the Tosi-Fumi potential. To analyze this in a quantitative way, we use the potassium chloride data at 295 °K under zero pressure (see Table VII).

In this case, the lattice-dynamic values underestimate the experimental C_{11}^T by 20%, and overestimate the experimental C_{12}^T and C_{44} by 40%. Since the calculations showed that 95% of C_{11}^T and 93% of C_{12}^T and C_{44} come from the static-lattice contributions, we need consider only these contributions in detail. They are further divided into contributions from individual parts (Coulomb, exponential repulsion, γ^{-6} and γ^{-8} attractions) in the Tosi-Fumi potential. These are given in Table VIII. Because the nearest-neighbor interactions make no contribution to C_{12}^0 , the repulsive potential can only weakly affect C_{12}^0 (superscript 0 represents the static-lattice contribution; see Table VIII). In fact, even if this term is neglected entirely, the theoretical value (6.9×10^{10} dyn cm⁻²)

TABLE VIII. Contributions of various (Coulomb, exponential repulsion, γ^{-6} , and γ^{-8} van der Waals attractions) parts of the Fumi-Tosi potential to the static-lattice properties of potassium chloride at lattice spacing 3.1462 Å.

	Coulomb	Repulsive	γ^{-6} attractive	γ^{-8} attractive	Total
Energy (10^{-12} erg per molecule)	-12.81	1.58	-0.46 (-0.84) ^a	-0.06	-11.76 (-12.14) ^a
Pressure (10^9 dyn cm ⁻²)	-68.57	80.28	-14.93 (-27.12)	-2.49	-5.71 (-17.89)
C_{11}^0 (10^{11} dyn cm ⁻²)	-3.69	8.15	-1.00 (-1.72)	-0.22	3.24 (2.52)
$C_{12}^0 = C_{44}^0$ (10^{11} dyn cm ⁻²)	0.82	0.17	-0.11 (-0.24)	-0.01	0.87 (0.74)

^aThese values are calculated from Lynch's values (Ref. 35) for the van der Waals dipole-dipole coefficients without local field corrections.

TABLE IX. The % rms displacements $\langle \Delta r^2 \rangle^{1/2}$ of alkali and halogen ions in an alkali-halide crystal, measured in units of the lattice spacings at 300 °K under zero pressure.

	$\langle \Delta r^2 \rangle^{1/2} / \langle \Delta r^2 \rangle^{1/2}$ (%)				
	Li ⁺	Na ⁺	K ⁺	Rb ⁺	Cs ⁺
F ⁻	6.56/6.21	6.65/6.95	6.32/7.04	5.97/6.73	5.29/5.81
Cl ⁻	6.16/5.96	6.24/6.31	5.84/5.93		
Br ⁻	6.57/6.23	6.08/6.08	6.09/6.15		
I ⁻	7.35/6.72	6.35/6.27	6.02/6.03		

still lies more than 10% above the experimental value (6.2×10^{10} dyn cm⁻²)! If one decides to keep the functional form of the Tosi-Fumi potential, both the repulsive and the attractive parameters in the potential have to be readjusted to reconcile with the deviations in C_{11}^T and C_{12}^T (or C_{44}). A readjusted potential must have a *stiffer* repulsion and a *stronger* van der Waals attraction between the (+, -) or (-, -) pair than the values given in Table I. An increased stiffness makes C_{11}^0 much larger without appreciably affecting C_{12}^0 , while a stronger r^{-6} attraction reduces C_{12}^0 (see Table VIII). In fact, recalculation of the van der Waals parameters by Lynch³⁵ indicates that the new values of c_{++} , c_{--} , and c_{+-} for potassium chloride can be larger than the old values by 170%, 57.5%, and -21%, respectively. Calculations using Lynch's values of c_{ij} 's are included in Table VIII. As expected, C_{12}^0 is improved appreciably. It would be useful to recalculate the parameters in the Tosi-Fumi potential by means of a suitable least-squares fit which uses, among other things, data on C_{12}^T (or C_{44}) as input values.

One can, of course, attribute the observed deviations to other effects than to the inadequacy of the pair potential, as we have done above. Available data are, however, not encouraging for such suggestions. The Axilrod-Teller triple-dipole potential contributes to C_{11}^T and C_{12}^T with the same sign.²⁵ This is also the case³⁶ for a noncentral potential, $c r^{-9}(x^4 + y^4 + z^4 - 0.6r^4)$, which is the first nonvanishing term in a multipole expansion of the electrostatic energy subject to the constraint of the cubic symmetry of the crystals. The shell-model values of C_{11}^0 , C_{12}^0 , and C_{44}^0 do not depend on the electronic polarizability³⁷ which we have neglected in our calculations. At this point, it may be useful to stress our view regarding the differences between the experimental and the theoretical Tosi-Fumi values of the elastic constants. A part of the differences might still be due to many-body effects of an unknown origin (to our knowledge, no satisfactory calculation of the elastic constants illustrating the deviations as a many-body effect has been published in open literature). Before attempting to make any quantitative calculation of this kind, we

take the view that it is necessary to know a more accurate expression for the pair potentials than those presently available. As we noted earlier, the use of an improved pair potential alone can reduce a large part of the observed deviations.

Root-Mean-Square Displacements

The ions in a crystal execute thermal and zero-point vibrations about their static-lattice positions. In general, the average magnitude of the displacement depends on the strength of the intermolecular force, the lattice structure, the ionic masses, the temperature, and the anharmonicity of the potential energy.

Table IX shows the rms displacements $\langle (\Delta r)^2 \rangle^{1/2}$ of alkali and halogen ions at 300 °K under zero pressure. The data are obtained by using the Tosi-Fumi potential in the harmonic cell model. The rms displacements of ions range from 5.3 to 7.4% of the lattice spacings. Except the fluoride salts, both alkali and halogen ions in a given alkali-halide crystal have about equal displacements. The anharmonic contributions reduce the rms displacements in Table IX by about 2%. However, their contribution becomes larger at higher temperatures. At the melting point, for example, $\langle \Delta r_K^2 \rangle^{1/2}$ and $\langle \Delta r_{Cl}^2 \rangle^{1/2}$ of potassium chloride are $0.124a$ and $0.125a$, respectively, and $\langle \Delta r_{Na}^2 \rangle^{1/2}$ and $\langle \Delta r_{Cl}^2 \rangle^{1/2}$ for sodium chloride are $0.128a$ and $0.125a$ ($a \equiv$ lattice spacing). The anharmonicity contributes about 8% of these values. It is interesting to note that the four values are close to each other. Lindemann³⁸ proposed that $\langle \Delta r^2 \rangle^{1/2}/a$ is nearly constant along the melting line. Experimental values of the rms displacements are not available for alkali halides. Since the cell-model restriction artificially inhibits a correlated motion of neighboring ions, the value (0.12–0.13) predicted here should be regarded as a lower limit to the Lindemann parameter of the alkali halides.

IV. SUMMARY AND CONCLUSIONS

We chose the interionic potential for alkali halides to be the Tosi-Fumi potential and computed the equilibrium properties by means of lattice dynamics and the LJD cell model. Comparison of the numerical data with available experimental data as well as those provided by the computer "experiments" enabled us to draw the following conclusions and to suggest several investigations worthy of being carried out in the future.

(i) Equations (13) and (14) provide reasonable and self-consistent ways of estimating the quantum and the anharmonic corrections, provided that these corrections are small. The anharmonic estimates of the elastic constants are not reliable. Further improvement can be obtained by using the correlated cell model,³⁹ where adjacent particles are

allowed to move together.

(ii) Discrepancies in the elastic constants are attributed to the softness in the repulsive core and the weakness in the van der Waals's attraction in the Tosi-Fumi potential. It would be worthwhile to improve the Tosi-Fumi potential by a least-squares fit to readjust the parameters in the potential.

(iii) The cell-model results for the anharmonic contributions suggest that the first two terms in a perturbation expansion of the anharmonic potential can nearly completely account for the observed anharmonic contributions. From a theoretical point of view, this result is encouraging, since the first two terms can be exactly evaluated though such calculations are tedious. The difficulty of evaluating the higher-order terms, however, increases very rapidly.

(iv) The elastic constants evaluated from the approximate theory of Leibfried *et al.* are different from those obtained from the exact lattice-dynamic calculations in qualitative and quantitative ways. The deviations occur in the way that the Einstein frequencies are defined for a *strained* lattice. The use of the Einstein frequencies introduced here for the strained lattice gives improved values of the elastic constants.

(v) It is probably not necessary to invoke many-body forces in order to explain the observed deviations from the Cauchy relations.

ACKNOWLEDGMENTS

We would like to thank W. G. Hoover for useful discussions and W. G. Cunningham for computational assistance.

*Work performed under the auspices of the U. S. Atomic Energy Commission.

- ¹B. Szigetti, *Trans. Faraday Soc.* **45**, 155 (1949); B. Szigetti, *Proc. R. Soc. A* **204**, 51 (1950).
- ²R. M. Lyddane and K. F. Herzfeld, *Phys. Rev.* **54**, 846 (1938).
- ³R. M. Lyddane, R. G. Sachs, and E. Teller, *Phys. Rev.* **59**, 673 (1941).
- ⁴L. C. Pauling, *The Nature of the Chemical Bond and the Structure of Molecules and Crystals*, 2nd ed. (Cornell U. P., Ithaca, N.Y., 1955).
- ⁵F. G. Fumi and M. P. Tosi, *J. Phys. Chem. Solids* **25**, 31 (1964); *J. Phys. Chem. Solids* **25**, 45 (1964).
- ⁶A. A. Maradudin, E. W. Montroll, G. H. Weiss, and I. P. Ipatova, *Theory of Lattice Dynamics in the Harmonic Approximations*, 2nd ed. (Academic, New York, 1971).
- ⁷See, for example, F. H. Ree, in *Physical Chemistry*, edited by H. Eyring, D. Henderson, and W. Jost (Academic, New York, 1971), Vol. 8A, p. 157.
- ⁸J. E. Lennard-Jones and A. F. Devonshire, *Proc. R. Soc. A* **163**, 53 (1938); *Proc. R. Soc. A* **167**, 1 (1938).
- ⁹E. R. Cowley, *J. Phys. C* **4**, 988 (1971).
- ¹⁰M. Arenstein, R. D. Hatcher, and J. Neuberger, *Phys. Rev.* **132**, 73 (1963).
- ¹¹L. V. Woodcock and K. Singer, *Trans. Faraday Soc.* **67**, 12 (1971).
- ¹²A. C. Holt, W. G. Hoover, S. G. Gray, and D. R. Shortle, *Physica (Utr.)* **49**, 61 (1970).
- ¹³A. C. Holt and M. Ross, *Phys. Rev. B* **1**, 2700 (1970).
- ¹⁴(a) D. A. McQuarrie, *J. Phys. Chem.* **66**, 1508 (1962); (b) G. L. Morley, *J. Chem. Phys.* **51**, 2336 (1969).
- ¹⁵G. Leibfried and H. Hahn, *Z. Phys.* **150**, 497 (1958).
- ¹⁶G. Leibfried and W. Ludwig, in *Solid State Physics*, edited by F. Seitz and D. Turnbull (Academic, New York, 1961), Vol. 12, p. 275.
- ¹⁷J. E. Mayer, *J. Chem. Phys.* **1**, 270 (1933).
- ¹⁸H. M. Evjen, *Phys. Rev.* **39**, 675 (1932).
- ¹⁹P. P. Ewald, *Ann. Phys. (N. Y.)* **21**, 1087 (1921).
- ²⁰B. R. A. Nijboer and F. W. de Wette, *Physica (Utr.)* **23**, 309 (1957).
- ²¹E. W. Kellermann, *Philos. Trans. R. Soc. Lond.* **238**, 513 (1940).
- ²²M. Born, *J. Chem. Phys.* **7**, 591 (1939).
- ²³See, for example, L. D. Landau and E. M. Lifshitz, *Statistical Physics* (Pergamon, London, 1958), p. 96.
- ²⁴W. G. Hoover, A. C. Holt, and D. R. Squire, *Physica (Utr.)* **44**, 437 (1969).
- ²⁵M. L. Klein and R. D. Murphy, *Phys. Rev. B* **6**, 2433 (1972).
- ²⁶V. V. Mitskevich, *Fiz. Tverd. Tela* **6**, 3020 (1964) [*Sov. Phys.-Solid State* **6**, 2405 (1965)].
- ²⁷B. N. N. Achar and T. R. Barsch, *Phys. Rev. B* **3**, 4352 (1971).
- ²⁸G. K. White, *Proc. R. Soc. A* **286**, 204 (1965).
- ²⁹G. K. White, in *Proceedings of the Eleventh International Conference on Low Temperature Physics*, edited by J. F. Allen, D. M. Finlayson, and D. M. McCall (University of St. Andrews Printing Dept., St. Andrews, Scotland, 1969), Vol. 1, p. 541.
- ³⁰T. H. K. Barron and A. Batana, *Phys. Rev.* **167**, 814 (1968).
- ³¹J. de Launay, *J. Chem. Phys.* **30**, 91 (1959).
- ³²W. B. Daniels, *Phys. Rev. Lett.* **8**, 3 (1962).
- ³³P. F. Choquard, *The Anharmonic Crystals* (Benjamin, New York, 1967).
- ³⁴A. J. Leadbetter, D. M. T. Newsham, and G. R. Settaree, *J. Phys. C* **2**, 393 (1969).
- ³⁵D. Lynch, *J. Phys. Chem. Solids* **28**, 1941 (1967).
- ³⁶Unpublished result obtained by one of us (A.C.H.).
- ³⁷R. A. Cowley, *Proc. R. Soc. A* **268**, 109 (1962); A. Herpin, *J. Phys. Radium* **14**, 611 (1953).
- ³⁸F. A. Lindemann, *Z. Phys.* **11**, 609 (1910).
- ³⁹D. R. Squire and Z. W. Salsburg, *J. Chem. Phys.* **35**, 486 (1961); B. J. Alder, W. G. Hoover, and T. E. Wainwright, *Phys. Rev. Lett.* **11**, 241 (1963).